Penerbit Akademia Baru

Journal of Advanced Research in Fluid Mechanics and Thermal Sciences

Journal homepage: www.akademiabaru.com/arfmts.html
ISSN: 2289-7879

The Effects of Convective and Porous Conditions on Peristaltic Transport of Non-Newtonian Fluid through a Non-Uniform Channel with Wall Properties

Open Access

Manjunatha Gudekote[1], Hanumesh Vaidya[2], Divya Baliga[1], Rajashekhar Choudhari[2,*], Kerehalli Vinayaka Prasad[2], Viharika[2]

[1] Department of Mathematics, Manipal Institute of Technology, Manipal Academy of Higher Education, Manipal, Karnataka, India
[2] Department of Mathematics, VSK University, Ballari, Karnataka, India

ARTICLE INFO

Article history:
Received 30 July 2019
Received in revised form 4 October 2019
Accepted 18 October 2019
Available online 10 November 2019

Keywords:
Biot number; concentration slip; wall properties; porous parameter; variable viscosity; variable thermal conductivity

ABSTRACT

In the present investigation, the effects of variable liquid properties along with wall properties are incorporated in the peristaltic mechanism of a Rabinowitsch fluid. The two-dimensional non-uniform channel is considered to be porous. The heat transfer characteristics are examined with convective conditions, whereas the mass transfer is considered with slip conditions at the walls. The model is developed with the assumptions of long wavelength and low Reynolds number. Exact solutions are obtained for velocity, streamlines, and concentration. Further, the perturbation technique is employed for obtaining the temperature solution. Moreover, the impact of relevant parameters on velocity, temperature, concentration, and streamlines are analysed for dilatant, Newtonian, and pseudoplastic fluid models. The variable liquid properties are found to enhance the fluid temperature for shear-thinning, shear thickening, and Newtonian fluids.

1. Introduction

The natural mechanism of a progressive wave of area contraction and relaxation in the human body which is responsible for many of the biological processes like the movement of food through the esophagus and chyme through the gastrointestinal tract is called peristalsis. Latham's [1] first investigations on peristalsis have led to its use in the modern day technology of dialysis machines, heart-lung machines, roller and finger pumps, etc. The concept of peristalsis has been studied and researched by many researchers on various fluids and geometries [2, 3]. Owing to the applications of heat transfer mechanisms during peristalsis in both thermal engineering and medical fields such as hemodialysis and cancer treatments, this field of research has garnered much attention in the past few years. Different parts of the human body are at different temperatures, which lead to the transfer

* *Corresponding author.*
E-mail address: choudhariraj3@gmail.com (Rajashekhar Choudhari)

of heat from elements at a higher temperature to the lower ones. The critical mode of heat transfer in the human body is convection. These convective boundary conditions have been incorporated by Alsaedi *et al.,* [4] by considering the Prandtl fluid with peristalsis. They observed that the Biot number has an increasing effect on the heat transfer coefficient and a decreasing impact on the temperature profiles. Joule heating and convective boundary conditions were used by Abbasi *et al.,* [5] in the study of peristaltic mechanism. Divya *et al.,* [6] have examined the peristalsis of a Herschel-Bulkley fluid with velocity and thermal conditions. They have also carried out examinations on the heat transfer of Jeffrey fluid model with convective boundary conditions in their study on the peristalsis through an elastic tube [7]. Of late, several researchers have investigated the heat transfer characteristics of biological fluids flowing through different geometries and with various assumptions [8-14].

The widespread applications of non-Newtonian fluid models in industrial and medical fields, as mentioned above, speaks a lot for the importance of non-Newtonian fluids over the Newtonian fluids. This has encouraged many researchers to consider the non-Newtonian models in their peristaltic studies. Among the many models studied, the analysis of the non-Newtonian behavior is claimed to be more accurate with the Rabinowitsch fluid model, after the hypothetical examination was experimentally verified by Wada and Hayashi [15]. The model was then utilized by Akbar and Nadeem [16] to the peristaltic transport through a uniform tube. Sadaf and Nadeem [17] further worked on peristaltic transport of Rabinowitsch fluid with combined viscous dissipation and convective effects. They observed that for all three cases of shear-thinning, shear-thickening, and viscous fluids, the Brinkman number plays a vital role in enhancing the fluid temperature. The investigation has been done by Vaidya *et al.,* [18] to study the heat transfer effects during the peristalsis of Rabinowitsch fluid flowing through a uniform inclined channel with compliant walls. Vaidya *et al.,* [19] researched the impact of convective and variable fluid properties on the peristaltic flow of Rabinowitsch fluid through a non-uniform tube. Manjunatha *et al.,* [20] have analysed the impact of heat and mass transfer on the Peristaltic mechanism of Jeffrey fluid through a non-uniform porous channel.

Over the recent few years, numerous researchers have paid more attention to the porous walls of the tube/channel in the physiological fluid flows. The major reason for this is due to the human lungs, gallbladder stones, blood vessels of small radius, etc. acting as a permeable media for fluid flow. The concept of permeable media was initially studied by Lukashey [21] in his investigations on peristaltic transport of fluid motion through porous capillary walls. Subsequently, El-Shehawey and Husseny [22] explored the peristaltic mechanism of a viscous incompressible fluid through the porous walls of a channel. Rao and Mishra [23] consolidated the Beavers-Joseph and Saffman boundary conditions to investigate the power-law fluid exhibiting the peristaltic motion in a porous tube. Vajravelu *et al.,* [24] considered the Casson fluid during the studies on the peristaltic flow through a porous walled circular tube along with Newtonian fluid. Their observations indicate that as the fluid turns more shear-thinned, the wall shear stress lessens. Several investigations accounting the effects of slip and porous media on the natural and biological fluids have been made [25-29].

Until recently, the thermophysical properties like viscosity and thermal conductivity of the fluid were considered to be constant in the studies on peristaltic mechanisms. But, in fluids like blood and other physiological liquids, these properties are not consistent and may vary. Accordingly, in such conditions, it is essential to consider the variable viscosity as well as variable thermal conductivity. Inspired by this, Srivastava *et al.,* [30] examined the peristalsis of a Newtonian fluid through uniform as well as non-uniform tubes with viscosity varying axisymmetrically. Studies on variable viscosity considerations were carried out by Khan *et al.,* [31] in their peristaltic studies on Jeffrey fluid through a porous media. Moreover, the consideration of variable thermal conductivity along with variable viscosity has garnered the attention of many researchers due to its widespread applications in the fields of medicine and industry. This has motivated Manjunatha *et al.,* [32, 33] to investigate the effects of varying viscosity and thermal conductivity during peristalsis of Casson and Bingham fluids under the considerations of convective and porous boundary conditions. Further, Vaidya *et al.,* [34-36] have carried out studies on Rabinowitsch fluid to study the effects of variable liquid properties on it under different geometrical considerations and assumptions.

The current paper deals with the influence of variable thermal conductivity and viscosity on the peristaltic mechanism of a non-Newtonian fluid. The fluid under consideration here is the Rabinowitsch fluid which flows through a two-dimensional non-uniform channel. Majority of the arteries, veins, and nerves are not horizontal but are inclined at a certain angle in the biological systems. Hence, the channel is considered to be inclined with respect to the horizontal surface. Also, the wall properties, along with the porous boundary conditions, are considered. Further, the heat and mass transfer characteristics are investigated with convective conditions and concentration slip, respectively. The closed-form solutions are obtained for velocity and concentration, whereas the temperature solution is obtained by the perturbation method. The graphs are plotted using MATLAB and are analysed for the effects of various parameters.

2. Mathematical Formulation and Closed Form Solutions

A Rabinowitsch fluid is considered to be flowing through an inclined non-uniform porous channel with complaint walls as shown in Figure 1. The angle of inclination of the channel with the horizontal surface is α . The sinusoidal wave trains are of wavelength λ which move along the walls of the channel with speed c . The geometry of the channel wall is given by [20]

$$\overline{H} = l(\overline{x}) + b\sin\left(\frac{2\pi}{\lambda}(\overline{x} - c\overline{t})\right), \tag{1}$$

where $l(\overline{x})$ is the non-uniform width of the channel, b is the wave amplitude and $\overline{t}$ is time.

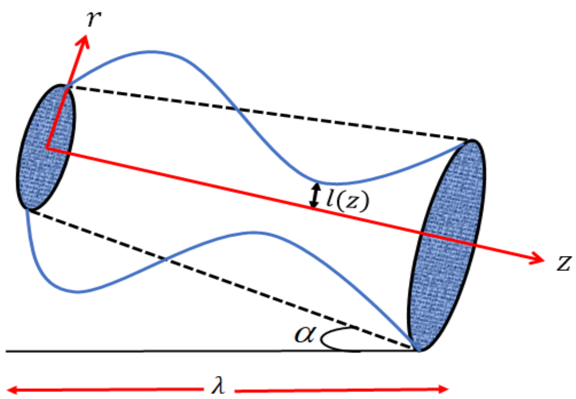

Fig. 1. Geometry of the model

The set of equations which govern the flow of the fluid are [20]

$$\frac{\partial \overline{u}}{\partial \overline{x}} + \frac{\partial \overline{w}}{\partial \overline{y}} = 0, \tag{2}$$

$$\rho\left(\frac{\partial \bar{u}}{\partial \bar{t}}+\bar{u}\frac{\partial \bar{u}}{\partial \bar{x}}+\bar{w}\frac{\partial \bar{u}}{\partial \bar{y}}\right)=-\frac{\partial \bar{p}}{\partial \bar{x}}+\frac{\partial \tau_{\bar{x}\bar{x}}}{\partial \bar{x}}+\frac{\partial \tau_{\bar{x}\bar{y}}}{\partial \bar{y}}+\rho g\sin\alpha\,, \tag{3}$$

$$\rho\left(\frac{\partial \bar{w}}{\partial \bar{t}}+\bar{u}\frac{\partial \bar{w}}{\partial \bar{x}}+\bar{w}\frac{\partial \bar{w}}{\partial \bar{y}}\right)=-\frac{\partial \bar{p}}{\partial \bar{y}}+\frac{\partial \tau_{\bar{x}\bar{x}}}{\partial \bar{x}}+\frac{\partial \tau_{\bar{x}\bar{y}}}{\partial \bar{y}}-\rho g\cos\alpha\,, \tag{4}$$

$$\rho c_p\left(\frac{\partial \bar{T}}{\partial \bar{t}}+\bar{u}\frac{\partial \bar{T}}{\partial \bar{x}}+\bar{w}\frac{\partial \bar{T}}{\partial \bar{y}}\right)=k\left(\frac{\partial^2 \bar{T}}{\partial \bar{x}^2}+\frac{\partial^2 \bar{T}}{\partial \bar{y}^2}\right)+\tau_{\bar{x}\bar{x}}\frac{\partial \bar{u}}{\partial \bar{x}}+\tau_{\bar{y}\bar{y}}\frac{\partial \bar{w}}{\partial \bar{y}}+\tau_{\bar{x}\bar{y}}\left(\frac{\partial \bar{w}}{\partial \bar{x}}+\frac{\partial \bar{u}}{\partial \bar{y}}\right), \tag{5}$$

$$\left(\frac{\partial \bar{C}}{\partial \bar{t}}+\bar{u}\frac{\partial \bar{C}}{\partial \bar{x}}+\bar{w}\frac{\partial \bar{C}}{\partial \bar{y}}\right)=D_1\left(\frac{\partial^2 \bar{C}}{\partial \bar{x}^2}+\frac{\partial^2 \bar{C}}{\partial \bar{y}^2}\right)+\frac{D_1 K'_T}{T'_m}\left(\frac{\partial^2 \bar{T}}{\partial \bar{x}^2}+\frac{\partial^2 \bar{T}}{\partial \bar{y}^2}\right), \tag{6}$$

where $\bar{u}, \bar{w}, \rho, p, \tau_{\bar{x}\bar{x}}, \tau_{\bar{x}\bar{y}}, \tau_{\bar{y}\bar{y}}, g, c_p, k, D_1, K'_T, T'_m, \bar{C}$ and $\bar{T}$ are the velocity component in radial direction, velocity component in axial direction, fluid density, pressure, extra stress tensor components, acceleration due to gravity, specific heat, thermal conductivity, mass diffusivity coefficient, thermal-diffusion ratio, mean temperature, fluid concentration and temperature respectively. The equation of the flexible wall motion is expressed as [18]

$$M(\bar{H})=\bar{p}-p_0\,. \tag{7}$$

where p_0 is the exterior pressure (taken to be 0 for simplicity) and M is an operator which is used to characterize the motion of the stretched membrane with damping forces and is given as

$$M=-\tau\frac{\partial^2}{\partial x^2}+e_1\frac{\partial^2}{\partial t^2}+e_2\frac{\partial}{\partial t}+e_3\frac{\partial^4}{\partial x^4}+H \tag{8}$$

where τ is the elastic tension of the membrane, e_1 is the mass per unit area, e_2 the coefficient of wall damping forces, e_3 is the flexural rigidity of the plate and H is the spring stiffness.

On using the continuity of stress at $y=h$ and the $x-$ component of the momentum equation, we obtain

$$\frac{\partial M(h)}{\partial x}=-\frac{\partial \bar{p}}{\partial \bar{x}}=\frac{\partial \tau_{\bar{x}\bar{x}}}{\partial \bar{x}}+\frac{\partial \tau_{\bar{x}\bar{y}}}{\partial \bar{y}}-\rho\left(\frac{\partial \bar{u}}{\partial \bar{t}}+\bar{u}\frac{\partial \bar{u}}{\partial \bar{x}}+\bar{w}\frac{\partial \bar{u}}{\partial \bar{y}}\right)+\rho g\sin\alpha\,. \tag{9}$$

The non-dimensional quantities are

$$x=\frac{\bar{x}}{l_2},y=\frac{\bar{y}}{\lambda},w=\frac{\bar{w}}{c},u=\frac{\lambda\bar{u}}{c\mu_0},\tau_{xx}=\frac{l_2\overline{\tau_{\bar{x}\bar{x}}}}{c\mu_0},\tau_{xy}=\frac{l_2\overline{\tau_{\bar{x}\bar{y}}}}{c\mu_0},\tau_{yy}=\frac{l_2\overline{\tau_{\bar{y}\bar{y}}}}{c\mu_0},Br=\frac{\eta c^2}{\bar{T}_0 l_2^2},$$
$$\varepsilon=\frac{b}{l_2},\delta=\frac{l_2}{\lambda},p=\frac{l_2^2\bar{p}}{c\lambda\mu_0},t=\frac{c\bar{t}}{\lambda},\mathrm{Re}=\frac{l_2 c\rho}{\mu_0},\theta=\frac{\bar{T}-\bar{T}_0}{\bar{T}_0},l(\bar{x})=l_2+k_1(\bar{x}),E_1=\frac{-\tau l_2^3}{\lambda^3\mu_0 c},$$
$$h=\frac{\bar{H}}{l_2}=1+\frac{\lambda k_1 z}{l_2}+\varepsilon\sin(2\pi(z-t)),E_2=\frac{e_1 l_2^3 c}{\lambda^3\mu_0},E_3=\frac{e_2 l_2^3}{\lambda^3\mu_0},F=\frac{\vartheta c}{g l_2^2},\mu_0=\frac{\bar{\mu}_0}{\mu},E_4=\frac{H l_2^3}{\lambda^5\mu_0 c},$$
$$E_5=\frac{H l_2^3}{\lambda\mu_0 c},\sigma=\frac{\bar{C}-C_0}{C_0},Sc=\frac{\mu}{\rho D_1},Sr=\frac{\rho D_1 K'_T T_0}{T'_m\mu_0 C_0},Bi=\frac{\eta l_2}{k}. \tag{10}$$

where Br is the Brinkmann number, ε is the amplitude ratio, δ is the wave number, p is pressure, Re is the Reynold's number, Bi is the Biot number, Sc and Sr are the Schmidt and Soret numbers, and E_1, E_2, E_3, E_4 and E_5 are the wall tension, mass characterization, wall damping, rigidity and wall elastic parameters respectively.

On using the above non-dimensional quantitates in Eq. (2)-(6), and considering the assumptions of long wavelength and low Reynolds number approximation, the resulting non-dimensional equations after dropping the bars are

$$\frac{\partial p}{\partial y}=0, \tag{11}$$

$$\frac{\partial p}{\partial x}=\frac{\partial\tau_{xy}}{\partial y}+\frac{\sin\alpha}{f}, \tag{12}$$

$$\frac{\partial}{\partial y}\left(k(\theta)\frac{\partial\theta}{\partial y}\right)+Br\,\tau_{xy}\frac{\partial u}{\partial y}=0, \tag{13}$$

$$\frac{\partial^2\sigma}{\partial y^2}+ScSr\frac{\partial^2\theta}{\partial y^2}=0. \tag{14}$$

where τ_{xy} is the constitutive equation of Rabinowitsch fluid and it is given by [30]

$$\tau_{xy}+\gamma\tau_{xy}^3=\mu(y)\frac{\partial u}{\partial y}, \tag{15}$$

where γ represents the pseudoplasticity coefficient and $\mu(y)$ represents the varying fluid viscosity given by

$$\mu(y)=1-\alpha_1 y,\quad \text{for } \alpha_1<<1, \tag{16}$$

α_1 being the coefficient of viscosity.
The thermal conductivity $k(\theta)$ is defined as

$$k(\theta)=1+\phi\theta, \quad \text{for} \quad \phi<<1 \tag{17}$$

where ϕ is the coefficient of thermal conductivity.
The corresponding non-dimensional boundary conditions are given by [20]

$$u=-1-\frac{\sqrt{Da}}{\beta}\frac{\partial u}{\partial y}\text{at } y=h=1+mx+\varepsilon\sin\left[2\pi(x-t)\right], \quad \frac{\partial u}{\partial y}=0 \quad \text{at} \quad y=0, \tag{18}$$

$$\frac{\partial\theta}{\partial y}+Bi\theta=0 \quad \text{at} \quad y=h, \qquad \frac{\partial\theta}{\partial y}=0 \quad \text{at} \quad y=0, \tag{19}$$

$$\sigma+\alpha_2\frac{\partial\sigma}{\partial y}=1 \quad \text{at} \quad y=h, \qquad \frac{\partial\sigma}{\partial y}=0 \quad \text{at} \quad y=0, \tag{20}$$

where Da is the Darcy number (porous parameter), m is the non-uniformity parameter, Bi is the Biot number and α_2 is the concentration slip parameter.

3. Solution Methodology

In order to get a solution for velocity field, Eq. (12), (13) and (17) are solved analytically with the help of boundary condition (18),

$$\begin{aligned} u=&\frac{(P-F)^3\gamma}{\alpha_1^{\,4}}\left[\log(1-h\alpha_1)-\log(1-y\alpha_1)\right]+\frac{(P-F)^3(h-y)\gamma}{\alpha_1^{\,3}}+\frac{(P-F)(h-y)}{\alpha_1}+\\ &\frac{(P-F)}{2\alpha_1^{\,2}}\left[(P-F)^2(h^2-y^2)\gamma+2\log(1-h\alpha_1)-2\log(1-y\alpha_1)\right]+\frac{(P-F)^3(h^3-y^3)\gamma}{3\alpha_1}-\\ &\frac{6\left[-\beta+h(F-P)\sqrt{Da}\left(1+h^2(P-F)^2\gamma\right)\right]+h\beta\alpha_1}{6\beta(-1+h\alpha_1)} \end{aligned} \tag{21}$$

where

$$P=\frac{\partial p}{\partial x}=8\varepsilon\pi^3\left(-(E_1+E_2)\cos(2\pi(x-t))+E_3\frac{\sin(2\pi(x-t))}{2\pi}+4\pi^2\left(E_4+\frac{E_5}{16\pi^4}\right)\cos(2\pi(x-t))\right),$$

$$F=\frac{\sin\alpha}{f}.$$

We now obtain the stream function from the following expression

$$u=\frac{\partial\psi}{\partial y}, \text{and } \psi=0 \text{ at } y=h, \tag{22}$$

which yields

$$\begin{aligned}\psi=&\frac{(F-P)^3\gamma\left(1+\log(1-h\alpha_1)-\log(1-y\alpha_1)\right)}{\alpha_1{}^5}-\frac{(F-P)^3 y\gamma\left(1+\log(1-h\alpha_1)-\log(1-y\alpha_1)\right)}{\alpha_1{}^4}+\\&\frac{3(P-F)^3(2h-y)y\gamma+6(P-F)\log(1-y\alpha_1)}{6\alpha_1{}^3}+\frac{(P-F)y\left(6+(F-P)^2(3h^2-y^2)\gamma\right)}{6\alpha_1{}^2}+\\&\frac{(P-F)y\left(\log(1-h\alpha_1)-\log(1-y\alpha_1)\right)}{\alpha_1{}^2}+\frac{6(F-P)y(-2h+y)+(F-P)^3y(-4h^3+y^3)\gamma}{12\alpha_1}+\\&\frac{y\left(\beta+h(P-F)\sqrt{Da}(1+h^2(F-P)^2\gamma)\right)}{\beta(-1+h\alpha_1)}-\frac{hy\alpha_1}{-1+h\alpha_1}\end{aligned} \tag{23}$$

It is not easy to find a closed form solution for Eq. (14) and (18). This difficulty is overcome by suitably using the small value of coefficient of thermal conductivity ($\phi<<1$) to obtain the perturbed solution for temperature. For this purpose, we write

$$\theta=\theta_0+\phi\theta_1+O\,(\phi^2). \tag{24}$$

The temperature function is obtained by the zeroth and first order solution of the above as:

$$\theta_0=\frac{-1}{60Bi\alpha_1{}^6}\left[\begin{aligned}&60Bi\,Br(F-P)^4\gamma(-\log(1-h\alpha_1)+\log(1-y\alpha_1))+60Br(F-P)^4\gamma\alpha_1\left((1+Bih)\log(1-h\alpha_1)-\right.\\&\left.Bi\left(h-y+y\log(1-y\alpha_1)\right)\right)+30Br\alpha_1{}^2(F-P)^2\left[(F-P)^2\gamma\left(2h+Bi\,h^2-Bi\,y^2\right)-2Bi\log(1-h\alpha_1)+\right.\\&\left.2Bi\log(1-y\alpha_1)\right]+10Br\alpha_1{}^3(F-P)^2\left[6Bi(-h+y)+(F-P)^2\gamma\left(3h^2+Bi\,h^3-Bi\,y^3\right)+\right.\\&\left.6(1+Bi\,h)\log(1-h\alpha_1)-6Bi\,y\log(1-y\alpha_1)\right]+5Br\alpha_1{}^4(F-P)^2\left[12h+6Bi\,h^2-6Bi\,y^2+\right.\\&\left.(F-P)^2\gamma\left(4h^3+4Bi\,h^4-Bi\,y^4\right)\right]+Br\alpha_1{}^5(F-P)^2\left[30h^2+10Bi\,h^3-10Bi\,y^3+\right.\\&\left.3(F-P)^2\gamma\left(5h^4+Bi\,h^5-Bi\,y^5\right)\right]-60\alpha_1{}^6\end{aligned}\right] \tag{25}$$

$$\theta_1 = \frac{-1}{3600 Bi^2 \alpha_1^{12}} \begin{bmatrix} 60 Bi\, Br(F-P)^4 \gamma(-\log(1-h\alpha_1)+\log(1-y\alpha_1)) + 60 Br(F-P)^4 \gamma\alpha_1\left((1+Bih)\log(1-h\alpha_1)-\right. \\ \left. Bi\left(h-y+y\log(1-y\alpha_1)\right)\right) + 30 Br\alpha_1^2 (F-P)^2\left[(F-P)^2\gamma\left(2h+Bi\,h^2-Bi\,y^2\right)-2Bi\log(1-h\alpha_1)\right. \\ \left. +2Bi\log(1-y\alpha_1)\right] + 10 Br\alpha_1^3 (F-P)^2\left[6Bi(-h+y)+(F-P)^2\gamma\left(3h^2+Bi\,h^3-Bi\,y^3\right)+\right. \\ \left. 6(1+Bi\,h)\log(1-h\alpha_1)-6Bi\,y\log(1-y\alpha_1)\right] + 5Br\alpha_1^4(F-P)^2\left[12h+6Bi\,h^2-6Bi\,y^2+\right. \\ \left. (F-P)^2\gamma\left(4h^3+4Bi\,h^4-Bi\,y^4\right)\right] + Br\alpha_1^5(F-P)^2\left[30h^2+10Bi\,h^3-10Bi\,y^3+\right. \\ \left. 3(F-P)^2\gamma\left(5h^4+Bi\,h^5-Bi\,y^5\right)\right] - 60\alpha_1^6 \end{bmatrix}^2 \quad (26)$$

Using the above in Eq. (24), we obtain the expression for temperature. The solution for concentration equation given by Eq. (14) along with Eq. (20) is found by utilizing Eq. (25) and (26) with the help of MATHEMATICA software.

4. Results and Discussion

In the current section, we discuss the graphical behavior of velocity, temperature and concentration profiles for the important parameters influencing them. Moreover, the phenomenon of trapping is also discussed. The values which are fixed in obtaining the graphs are $m = 0.05, \varepsilon = 0.6, Da = 0.02, \alpha = \frac{\pi}{4}, \beta = 0.2, \alpha_1 = 0.02, \phi = 0.02, E_1 = 0.1, E_2 = 0.04, E_3 = 0.4, E_4 = 0.002$ and $E_5 = 0.01.$

4.1 Velocity Fields

The influence of variable viscosity α_1, Darcy number Da, velocity slip parameter β, angle of inclination α and the non-uniform parameter m are illustrated in Figure 2(a)-2(e). Each of these parameters are studied for their influence on velocity considering dilatant/shear thickening ($\gamma < 0$), Newtonian/viscous ($\gamma = 0$) and pseudoplastic/shear thinning ($\gamma > 0$) cases of the Rabinowitsch model. These figures clearly exhibit the parabolic profile for velocity. The variable viscosity is seen to accelerate the fluid motion for shear thickening as well as viscous fluids. However, with an increase in α_1, the fluid velocity along the axial direction diminishes for a shear thickening fluid (as shown in Figure 2(a)). From Figure 2(b), it can be observed that fluid velocity of the dilatant and Newtonian cases is enhanced with increasing porosity of the channel, whereas the decrease in the porous parameter Da is responsible for a rise in the fluid velocity for pseudoplastic fluids. The impact of velocity slip parameter β is seen to be exactly the opposite as compared to Da. This nature can be seen in Figure 2(c). The larger the inclination of the channel, the faster the dilatant and Newtonian fluid moves, and slower motion of the shear-thinning fluid, as observed from Figure 2(d). Also, as the channel becomes more non-uniform, the velocity of the dilatant and Newtonian fluid rises and that of the pseudoplastic fluid reduces (as shown in Figure 2(e)). To observe the effects of changes in the wall properties on the fluid velocity, Figure 3(a)-3(c) are plotted. From Figure 3(a), it can be noted that in the case of a dilatant fluid, an increase in the values of E_1 and E_2 leads to an increase in the fluid velocity but higher values of E_3, E_4 and E_5 diminishes it. Contrasting influence of these parameters is seen on Newtonian (Figure 3(b)) and pseudoplastic fluids (Figure 3(c)).

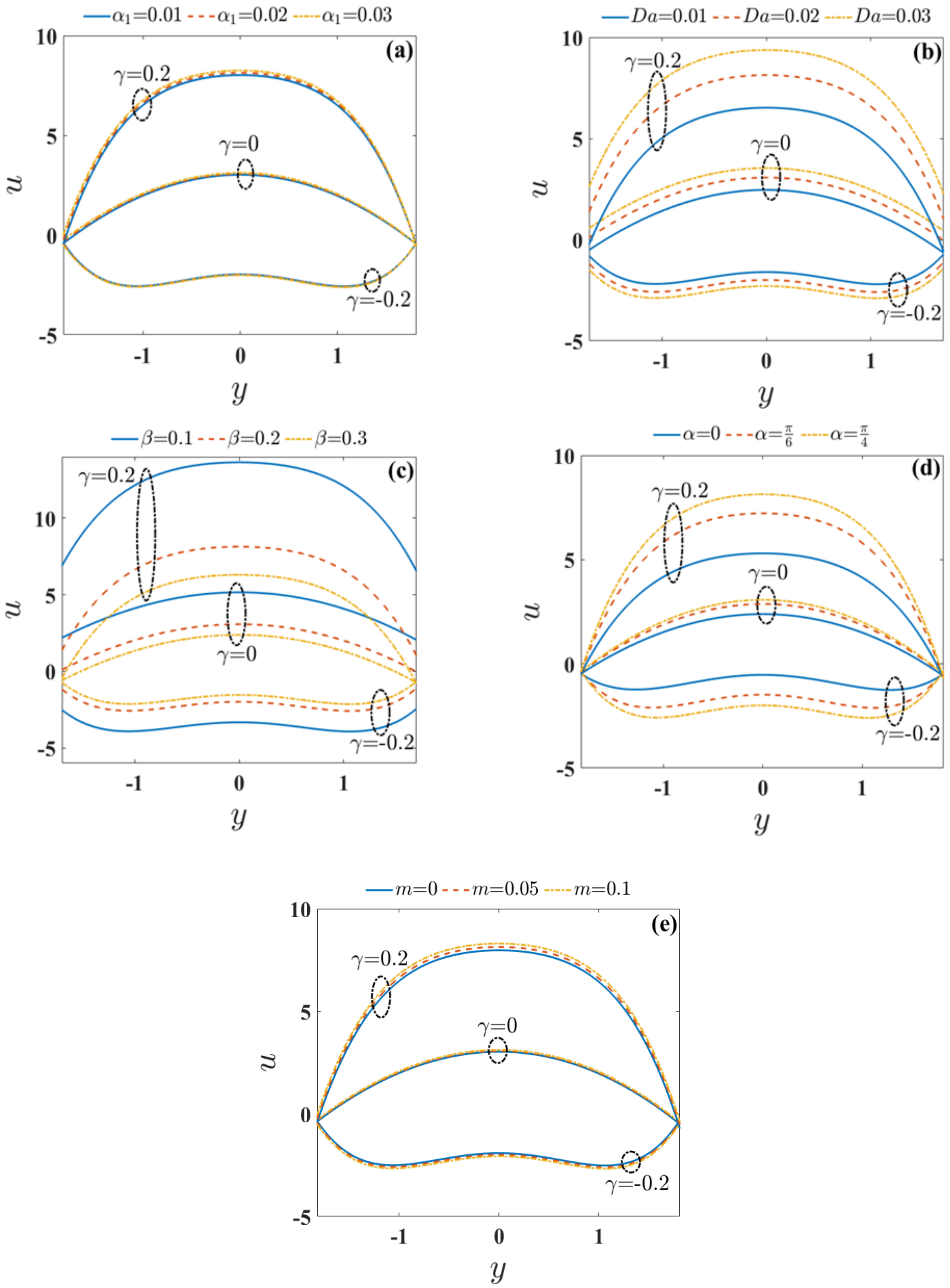

Fig. 2. Velocity profiles for varying (a) α_1, (b) Da, (c) β, (d) α and (e) m with $\gamma = -0.2, 0, 0.2$

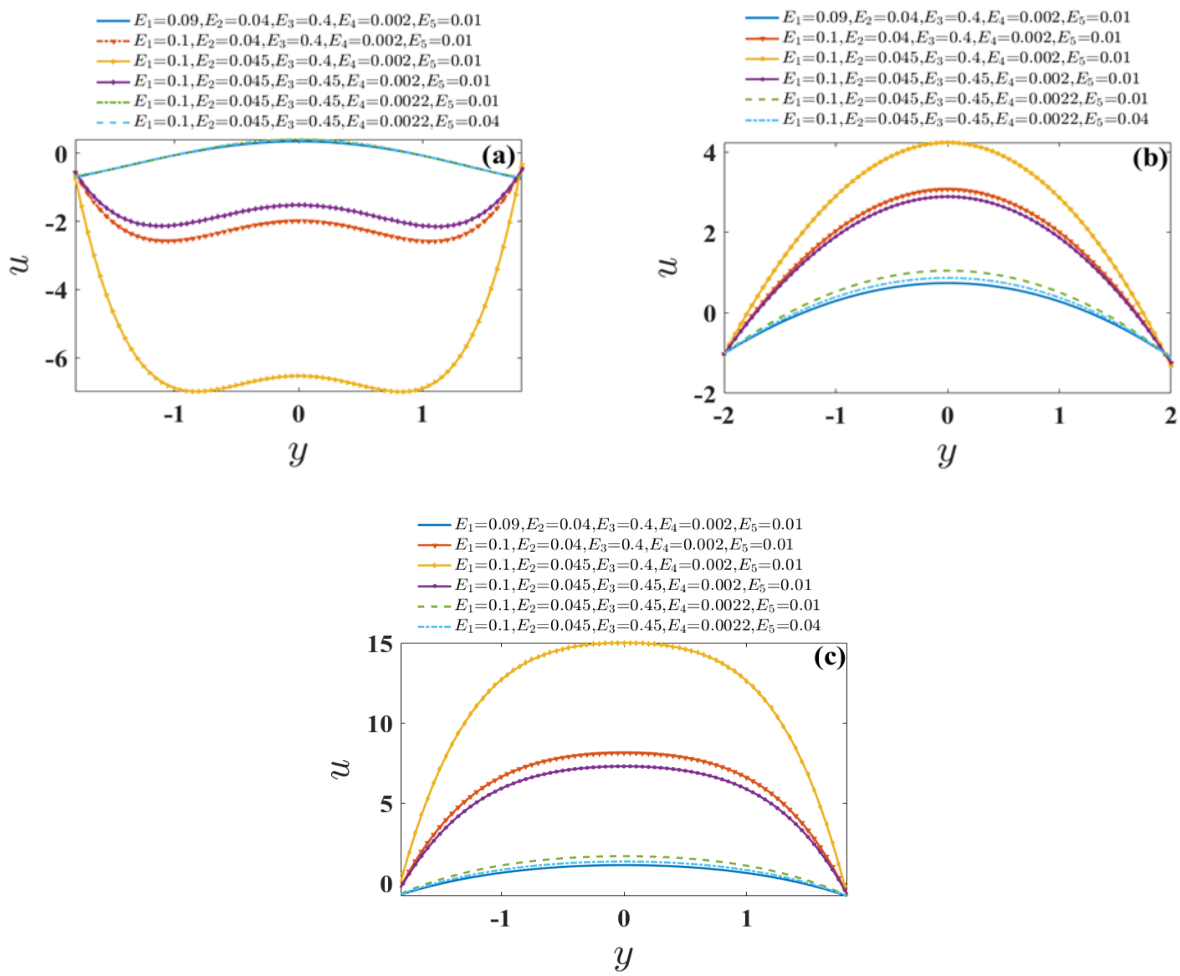

Fig. 3. Velocity profiles for varying wall properties with (a) $\gamma = -0.2$, (b) $\gamma = 0$ and (c) $\gamma = 0.2$

4.2 Temperature and Concentration Profiles

The effects of the pertinent parameters on the nature of temperature profiles are studied through Figure 4-9, where we consider the parameter of variable viscosity α_1, variable thermal conductivity ϕ, non-uniformity parameter m, Biot number Bi, Brinkman number Br and the angle α by which the channel is inclined. These graphs are plotted for the three different cases of the Rabinowitsch fluid model. As the variable viscosity of the fluid α_1 increases, Figure 4 shows that the fluid temperature also gets enhanced. The ability of the fluid particles to hold or disperse the heat to its environment gets enhanced for higher values of ϕ. This results in a higher temperature of the fluid than its boundary, irrespective of the fluid nature. This behavior is clearly illustrated in Figure 5. Likewise, the fluid temperature is seen to increase for higher values of the non-uniformity parameter m (as shown in Figure 6). However, from Figure 7 it can be observed that with an increase in the magnitude of Bi, the fluid temperature falls for all the three types of fluids. This nature is because the Biot number plays a significant role in thermal conductivity of the fluid. Hence, higher values of Bi results in a drop in the fluid thermal conductivity, thus reducing its temperature. An opposite influence of Br can be seen in Figure 8. The increasing effect of the angle of inclination on the fluid temperature for dilatant, Newtonian and pseudoplastic fluids is depicted in Figure 9. The impact of the wall properties on temperature profile can be seen from the plots in Figure 10(a)-(c). For shear-thickening fluids, the temperature profile sees an enhancement for E_1 and E_2, whereas the temperature drops for E_3, E_4 and E_5 (as shown in Figure 10(a)). Figure 10(b) and 10(c) also show a similar influence of the wall properties on viscous and shear-thinning fluids respectively.

The ramifications of concentration slip parameter α_2, Schmidt number Sc and Soret number Sr on mass transfer characteristics of shear-thickening, Newtonian and shear-thinning fluids are depicted in Figure 11-13. For all the three cases of the Rabinowitsch model, the concentration of fluid particles are found to increase near the lower wall and decrease near the upper wall for higher values of α_2, whereas no difference in the fluid concentration is observed in the central part of the channel (as shown in Figure 11). From Figure 12 and 13, higher values of Schmidt and Soret numbers are seen to decrease the fluid concentration irrespective of dilatant, Newtonian and pseudoplastic fluids.

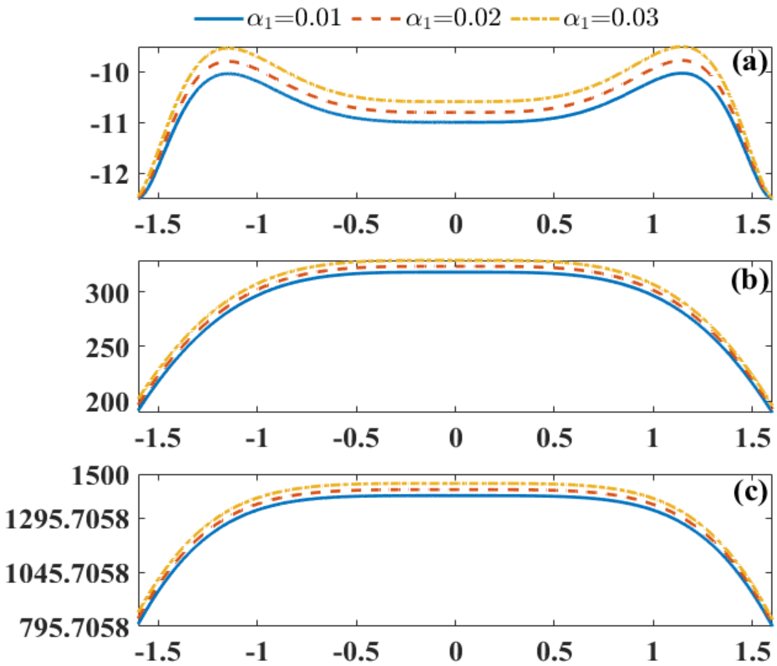

Fig. 4. Temperature profiles for varying α_1 with (a) $\gamma = -0.0005$, (b) $\gamma = 0$ and (c) $\gamma = 0.0005$

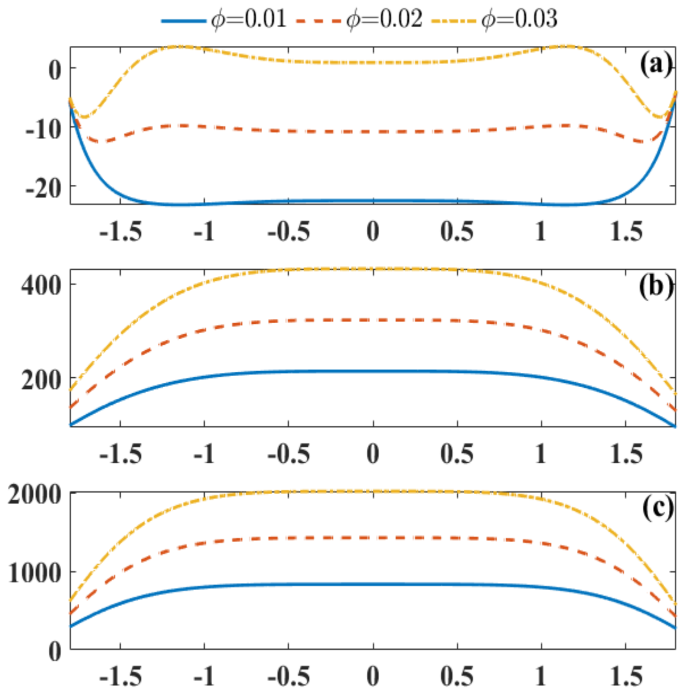

Fig. 5. Temperature profiles for varying ϕ with (a) $\gamma = -0.0005$, (b) $\gamma = 0$ and (c) $\gamma = 0.0005$

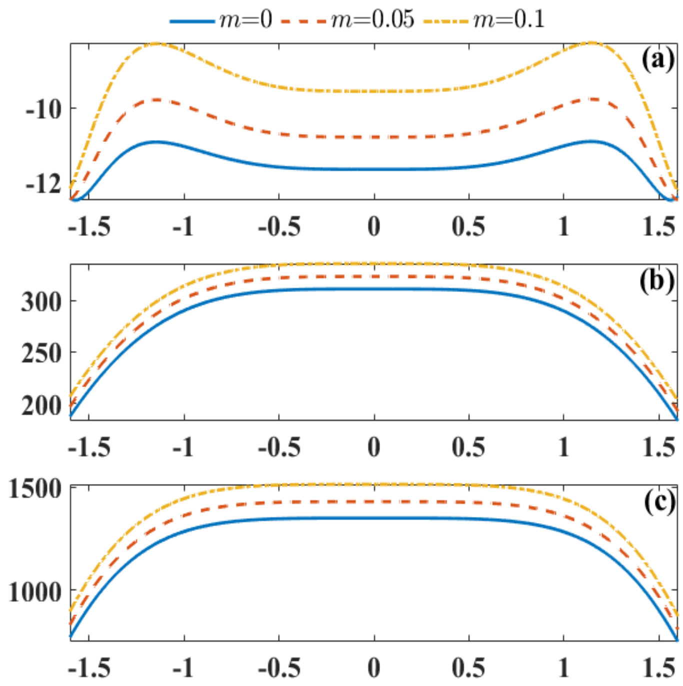

Fig. 6. Temperature profiles for varying m with (a) $\gamma = -0.0005$, (b) $\gamma = 0$ and (c) $\gamma = 0.0005$

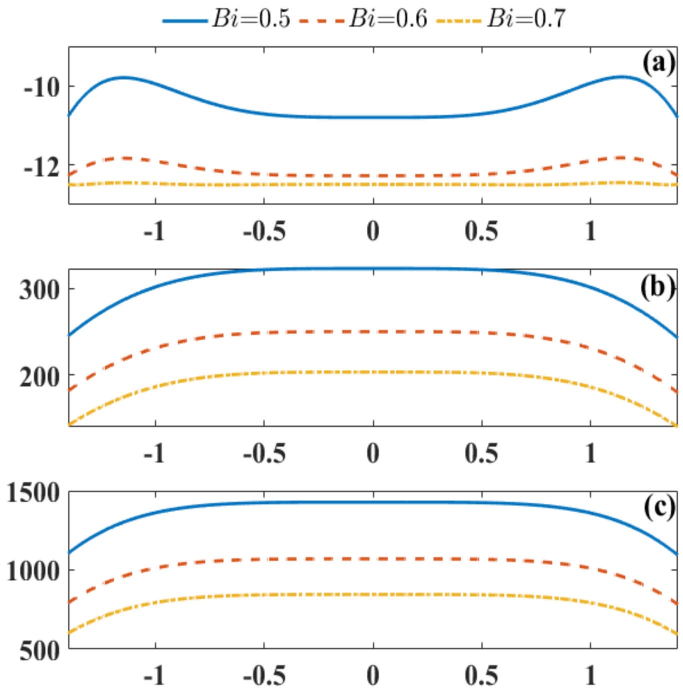

Fig. 7. Temperature profiles for varying Bi with (a) $\gamma = -0.0005$, (b) $\gamma = 0$ and (c) $\gamma = 0.0005$

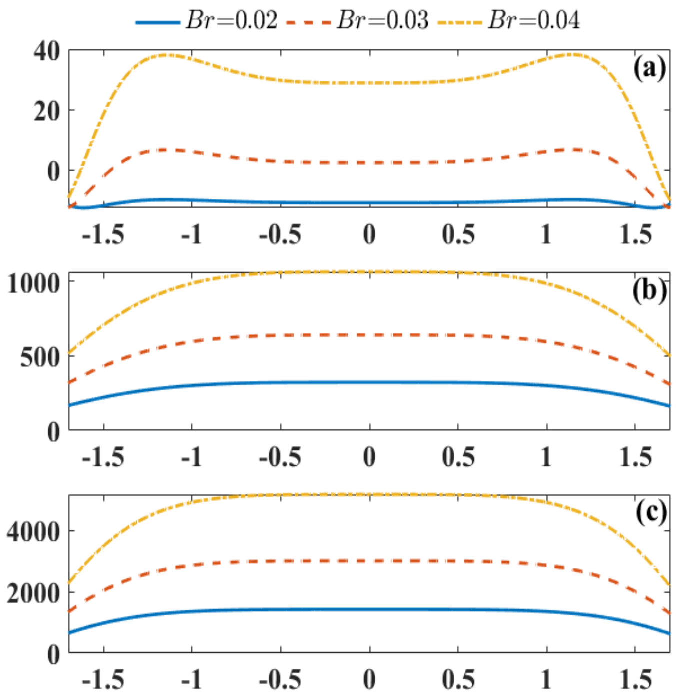

Fig. 8. Temperature profiles for varying Br with (a) $\gamma = -0.0005$, (b) $\gamma = 0$ and (c) $\gamma = 0.0005$

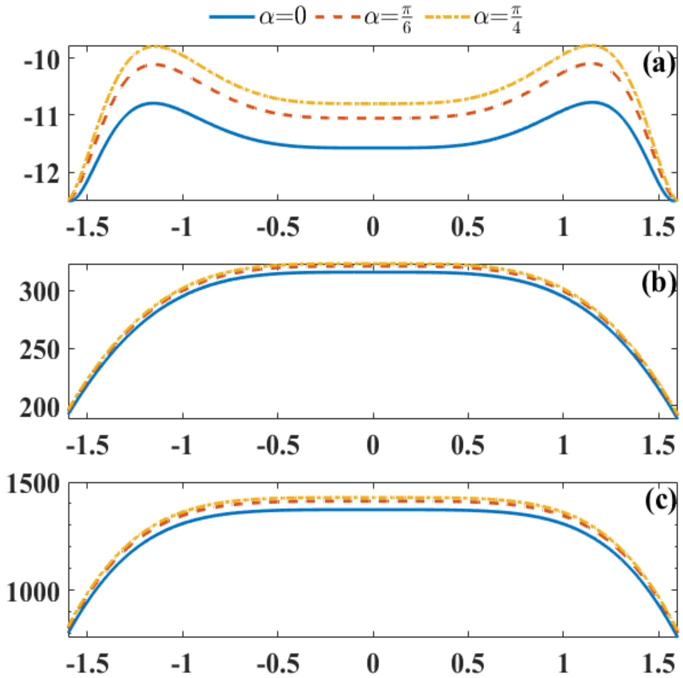

Fig. 9. Temperature profiles for varying α with (a) $\gamma = -0.0005$, (b) $\gamma = 0$ and (c) $\gamma = 0.0005$

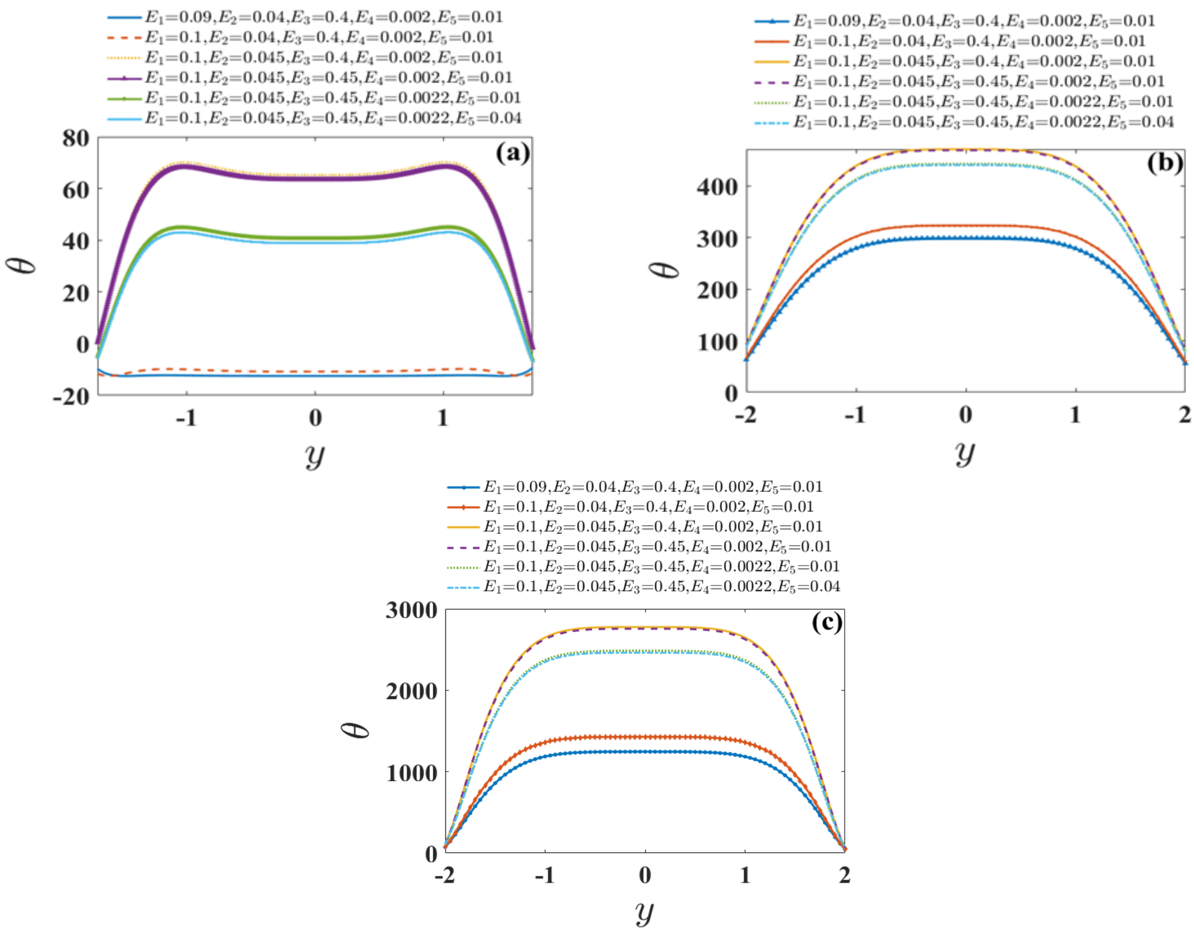

Fig. 10. Temperature profiles for varying wall properties with (a) $\gamma = -0.0005$, (b) $\gamma = 0$ and (c) $\gamma = 0.0005$

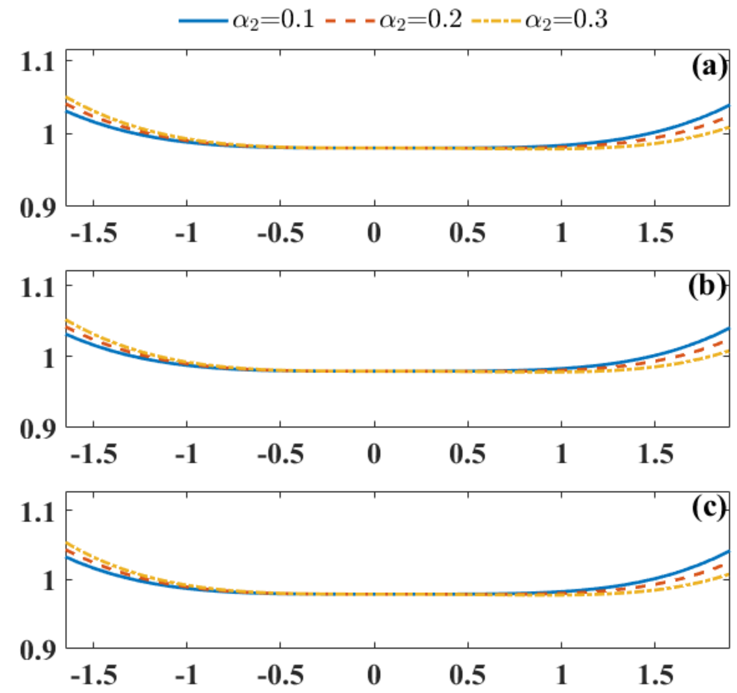

Fig. 11. Concentration profiles for varying α_2 with (a) $\gamma = -0.0005$, (b) $\gamma = 0$ and (c) $\gamma = 0.0005$

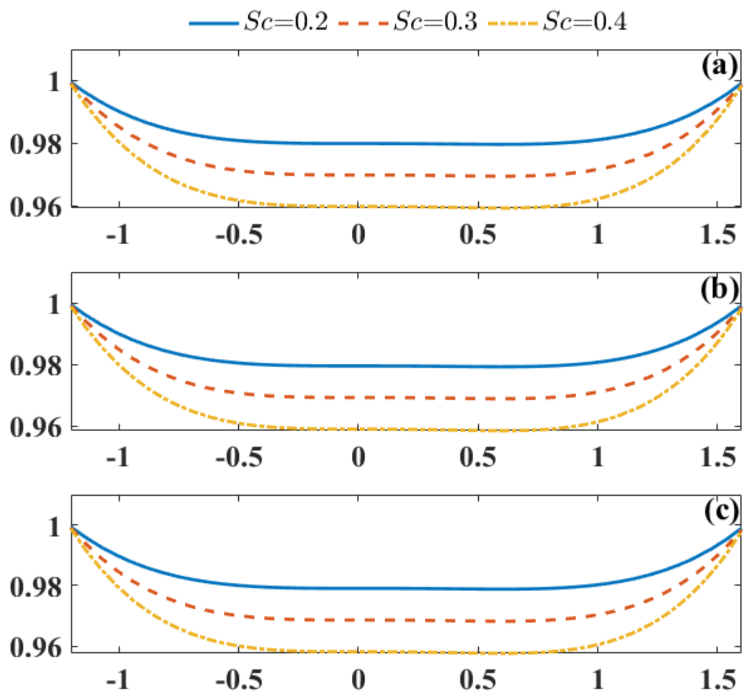

Fig. 12. Concentration profiles for varying Sc with (a) $\gamma = -0.0005$, (b) $\gamma = 0$ and (c) $\gamma = 0.0005$

Journal of Advanced Research in Fluid Mechanics and Thermal Sciences
Volume 63, Issue 1 (2019) 52-71

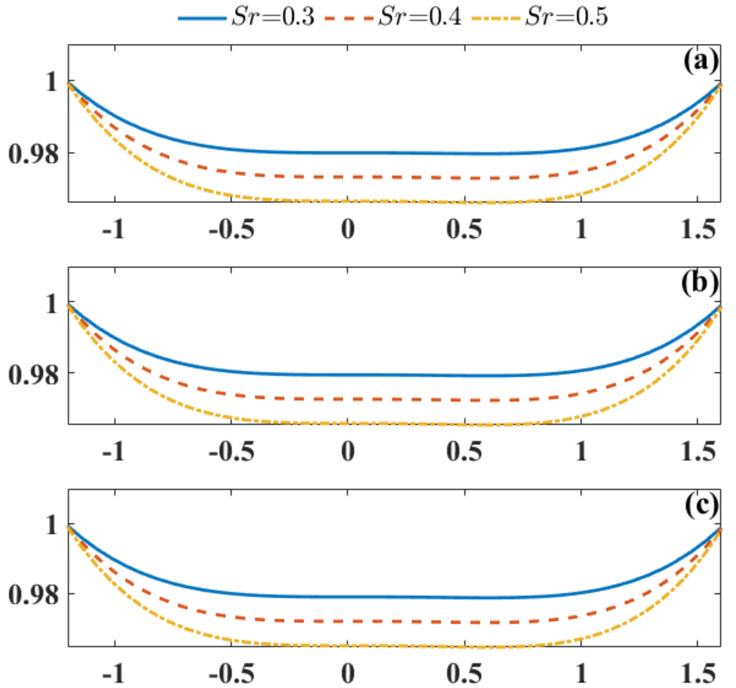

Fig. 13. Concentration profiles for varying Sr with (a) $\gamma = -0.0005$, (b) $\gamma = 0$ and (c) $\gamma = 0.0005$

4.3 Trapping Phenomenon

The most important topic of discussion in studies on peristaltic transport is the phenomenon of trapping which results in bolus formation. This bolus moves forward along with the sinusoidal waves of peristaltic mechanism. This section focuses on the trapping phenomenon for variation in the variable viscosity parameter α_1, porous parameter Da and the non-uniformity parameter m on all three fluid cases. For this purpose, the contour plots, as shown in Figure 14-16 are drawn. For an increase in α_1, the size of the bolus trapped increases for shear-thickening as well as shear-thinning fluids (as shown in Figure 14(a)-(b) and Figure 14(e)-(f)). However, the trend is reversed for a Newtonian fluid (as shown in Figure 14(b)-(c)). From Figure 15(a)-(f), it can be noticed that for all the three types of fluids, the size of the trapped bolus increases for higher values of the porous parameter Da. A similar impact of the non-uniformity parameter is seen on the trapping phenomenon in Figure 16(a)-(f), where the bolus size increases as the channel becomes more non-uniform.

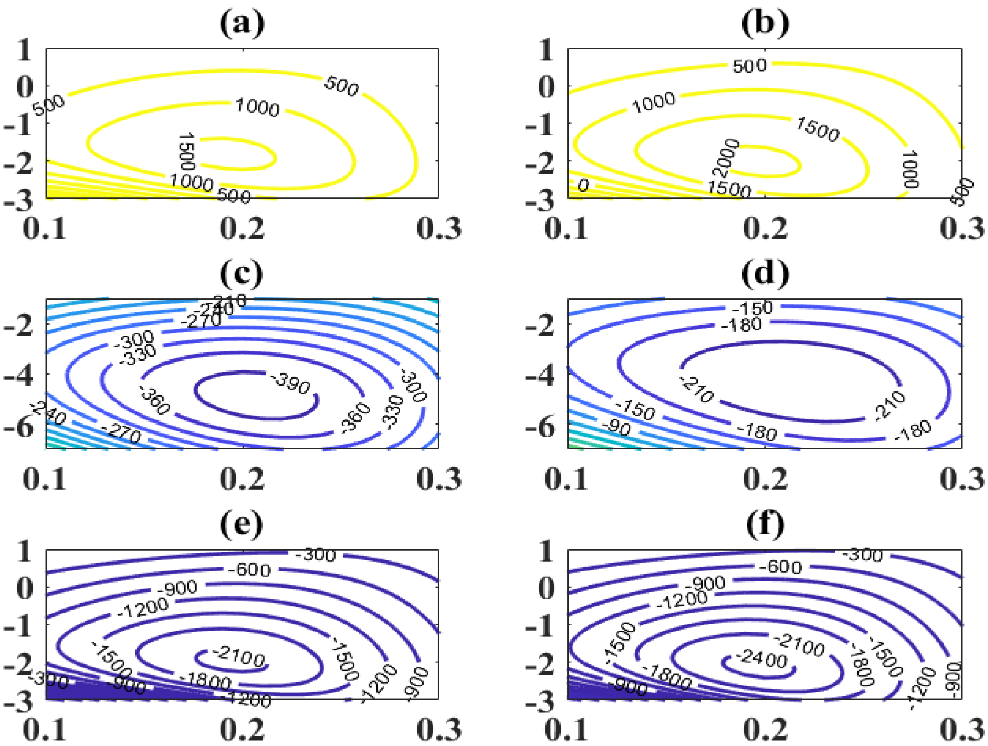

Fig. 14. Bolus for varying α_1 with (a) $\alpha_1 = 0.01,\ \gamma = -0.2$, (b) $\alpha_1 = 0.02,\ \gamma = -0.2$, (c) $\alpha_1 = 0.01,\ \gamma = 0$, (d) $\alpha_1 = 0.02,\ \gamma = 0$, (e) $\alpha_1 = 0.01,\ \gamma = 0.2$ and (f) $\alpha_1 = 0.02,\ \gamma = 0.2$

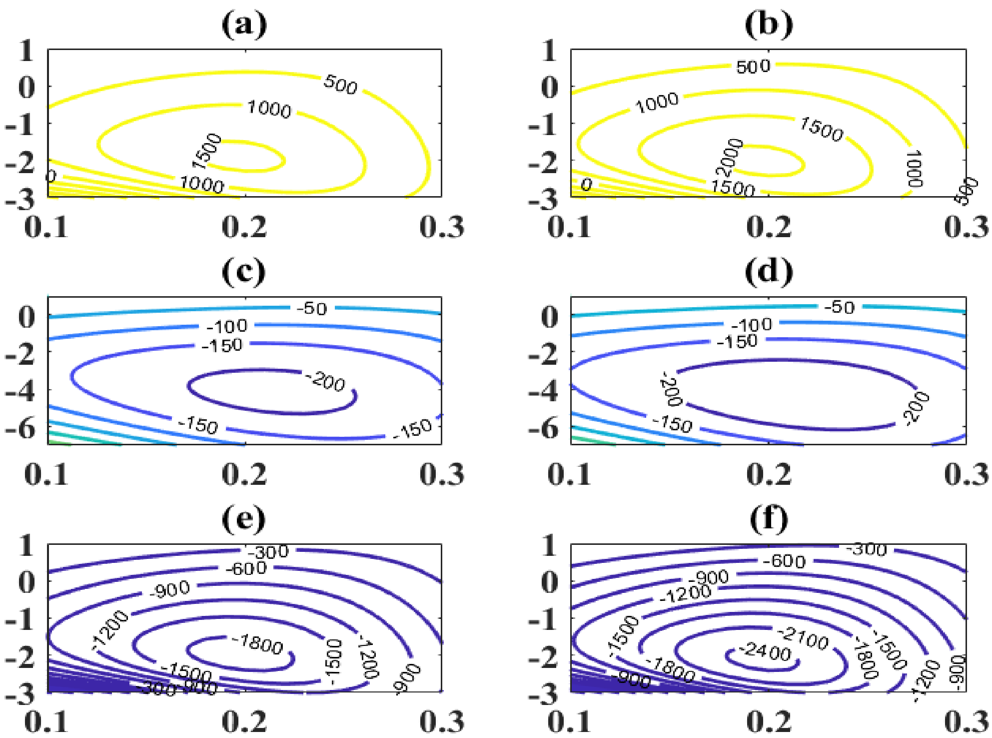

Fig. 15. Bolus for varying Da with (a) $Da = 0.01,\ \gamma = -0.2$, (b) $Da = 0.02,\ \gamma = -0.2$, (c) $Da = 0.01,\ \gamma = 0$, (d) $Da = 0.02,\ \gamma = 0$, (e) $Da = 0.01,\ \gamma = 0.2$ and (f) $Da = 0.02,\ \gamma = 0.2$

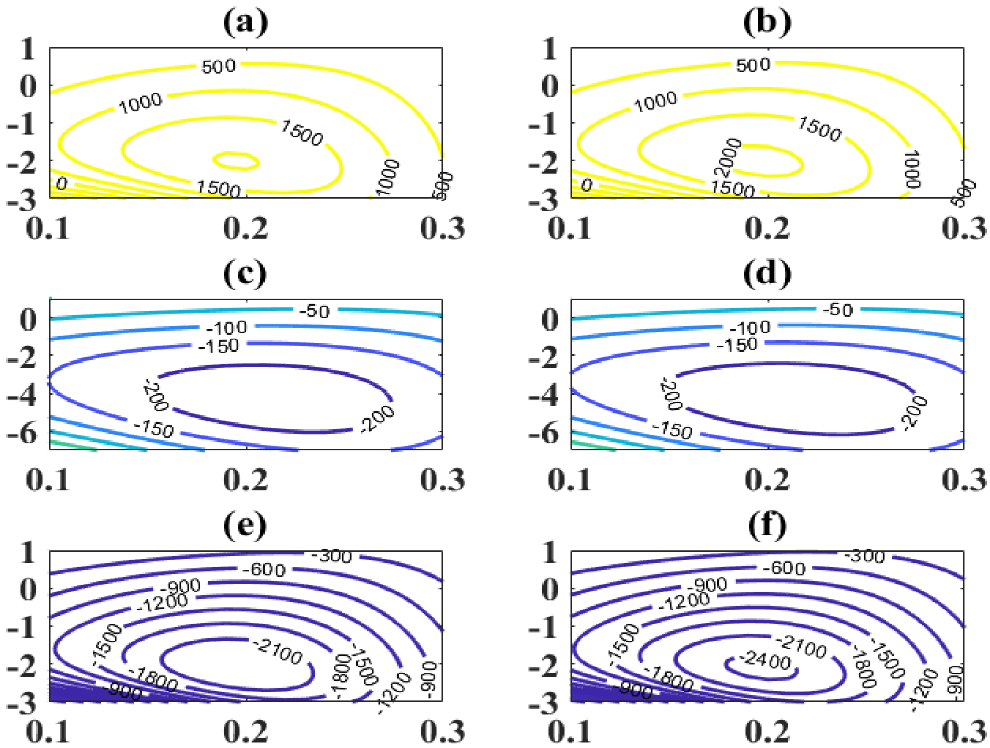

Fig. 16. Bolus for varying m with (a) $m=0,\ \gamma=-0.2$, (b) $m=0.05,\ \gamma=-0.2$, (c) $m=0,\ \gamma=0$, (d) $m=0.05,\ \gamma=0$, (e) $m=0,\ \gamma=0.2$ and (f) $m=0.05,\ \gamma=0.2$

5. Conclusions

The present investigation attempts to examine the peristaltic mechanism of a non-Newtonian fluid with heat and mass transfer mechanisms along with wall properties. The channel through which the fluid flows is taken to be non-uniform, inclined and porous. Also the convective and concentration slip conditions are considered. Further, the Rabinowitsch fluid model is considered with variable fluid properties. Analytical solutions are obtained for velocity and concentration fields, while perturbation technique is employed for obtaining the solution for temperature equation. The results are obtained for all the three cases of the Rabinowitsch model, namely dilatant/shear thickening fluid ($\gamma<0$), Newtonian/viscous fluid ($\gamma=0$) and pseudoplastic/shear thinning fluid ($\gamma>0$). The major findings of the study are

i. Variable viscosity, inclination angle, porous and non-uniformity parameters play a significant role in the enhancement of the fluid velocity of dilatant and pseudoplastic fluids.
ii. For pseudoplastic fluids, a rise in velocity occurs for smaller values of variable viscosity and non-uniformity parameter, and for large values of the velocity-slip parameter.
iii. The fluid temperature rises with variable liquid properties and Brinkman number.
iv. Higher values of Biot number lead to a drop in the temperature of the fluid.
v. Increase in the value of Brinkmann number enhances the temperature profile.
vi. Schmidt and Soret numbers have a decreasing effect on the concentration profile for all types of fluids.
vii. The parameters E_1 and E_2 decrease the velocity of dilatant fluids, whereas the temperature of Newtonian and pseudoplastic fluids increase.

viii. The size of boluses formed during peristalsis gets magnified with non-uniformity and porous parameters for all types of fluids.
ix. The size of trapped bolus diminishes for an increase in the value of variable viscosity for Newtonian fluid.

Acknowledgement
The authors appreciate the constructive comments of the reviewers which led to definite improvement in the paper.

References
[1] Latham, Thomas Walker. "Fluid motions in a peristaltic pump." PhD diss., Massachusetts Institute of Technology, 1966.
[2] Misra, J. C., and S. K. Pandey. "Peristaltic transport of blood in small vessels: study of a mathematical model." *Computers & Mathematics with Applications* 43, no. 8-9 (2002): 1183-1193.
[3] Mishra, Manoranjan, and A. Ramachandra Rao. "Peristaltic transport of a Newtonian fluid in an asymmetric channel." *Zeitschrift für angewandte Mathematik und Physik ZAMP* 54, no. 3 (2003): 532-550.
[4] Alsaedi, A., Naheed Batool, H. Yasmin, and T. Hayat. "Convective heat transfer analysis on Prandtl fluid model with peristalsis." *Applied Bionics and Biomechanics* 10, no. 4 (2013): 197-208.
[5] Munir, Abbasi Fahad, Hayat Tasawar, and Ahmad Bashir. "Peristaltic flow in an asymmetric channel with convective boundary conditions and Joule heating." *Journal of Central South University* 21, no. 4 (2014): 1411-1416.
[6] Baliga, Divya, Manjunatha Gudekote, Rajashekhar Choudhari, Hanumesh Vaidya, and Kerehalli Vinayaka Prasad. "Influence of velocity and thermal slip on the peristaltic transport of a Herschel-Bulkley fluid through an inclined porous tube." *Journal of Advanced Research in Fluid Mechanics and Thermal Sciences* 56, no. 2 (2019): 195-210.
[7] Divya, B., G. Manjunatha, C. Rajashekhar, Vaidya Hanumesh, and K. Prasad. "Impact of variable liquid properties on Peristaltic mechanism of convectively heated Jeffrey fluid in a slippery elastic tube." *Frontiers in Heat and Mass Transfer (FHMT)* 12, no 15 (2018): 1-9.
[8] Mebarek-oudina, Fateh, and Rachid Bessaïh. "Numerical modeling of MHD stability in a cylindrical configuration." *Journal of the Franklin Institute* 351, no. 2 (2014): 667-681.
[9] Hayat, T., Z. Nisar, H. Yasmin, and A. Alsaedi. "Peristaltic transport of nanofluid in a compliant wall channel with convective conditions and thermal radiation." *Journal of Molecular Liquids* 220 (2016): 448-453.
[10] Mebarek-Oudina, Fateh, and R. Bessaih. "Oscillatory magnetohydrodynamic natural convection of liquid metal between vertical coaxial cylinders." *J. Appl. Fluid Mech* 9, no. 4 (2016): 1655-1665.
[11] Wakif, A., Boulahia, Z., & Sehaqui, R. (2018). A semi-analytical analysis of electro-thermo-hydrodynamic stability in dielectric nanofluids using Buongiorno's mathematical model together with more realistic boundary conditions. *Results in Physics*, *9*, 1438-1454.
[12] Wakif, Abderrahim, Zoubair Boulahia, S. R. Mishra, Mohammad Mehdi Rashidi, and Rachid Sehaqui. "Influence of a uniform transverse magnetic field on the thermo-hydrodynamic stability in water-based nanofluids with metallic nanoparticles using the generalized Buongiorno's mathematical model." *The European Physical Journal Plus* 133, no. 5 (2018): 181.
[13] Choudhari, Rajashekhar, Manjunatha Gudekote, and Naveen Choudhari. "Analytical solutions on the flow of blood with the effects of Hematocrit, Slip and TPMA in a porous tube." *Journal of Advanced Research in Fluid Mechanics and Thermal Sciences* 47, no. 1 (2018): 201-208.
[14] Choudhari, Rajashekhar, Manjunatha Gudekote, Hanumesh Vaidya, and Kerehalli Vinayaka Prasad. "Peristaltic flow of Herschel-Bulkley fluid in an elastic tube with slip at porous walls." *Journal of Advanced Research in Fluid Mechanics and Thermal Sciences* 52, no. 1 (2018): 63-75.
[15] Wada, Sanae, and Hirotsugu Hayashi. "Hydrodynamic lubrication of journal bearings by pseudo-plastic lubricants: part 1, theoretical studies." *Bulletin of JSME* 14, no. 69 (1971): 268-278.
[16] Akbar, Noreen Sher, and Sohail Nadeemb. "Application of rabinowitsch fluid model in peristalsis." *Zeitschrift für Naturforschung A* 69, no. 8-9 (2014): 473-480.
[17] Sadaf, Hina, and Sohail Nadeem. "Analysis of combined convective and viscous dissipation effects for peristaltic flow of Rabinowitsch fluid model." *Journal of Bionic Engineering* 14, no. 1 (2017): 182-190.
[18] Vaidya, Hanumesh, C. Rajashekhar, G. Manjunatha, and K. V. Prasad. "Rheological properties and peristalsis of Rabinowitsch fluid through compliant porous walls in an inclined channel." *Journal of Nanofluids* 8, no. 5 (2018): 970-979.

[19] Vaidya, Hanumesh, Rajashekhar Choudhari, Manjunatha Gudekote, Kerehalli Vinayaka Prasad, Oluwole Daniel Makinde, and S. Sreenadh. "Peristaltic Motion of Non-Newtonian Fluid with Variable Liquid Properties in a Convectively Heated Non-Uniform Tube: Rabinowitsch Fluid Model." *Journal of Enhanced Heat Transfer* 26, no. 3 (2019): 277-294.
[20] Manjunatha, G., C. Rajashekhar, Hanumesh Vaidya, K. V. Prasad, and K. Vajravelu. "Impact of heat and mass transfer on the peristaltic mechanism of Jeffery fluid in a non-uniform porous channel with variable viscosity and thermal conductivity." *Journal of Thermal Analysis and Calorimetry* (2019): 1-16.
[21] Lukashev, E. A. "Mathematical model of the peristaltic transport of liquid initiated by the auto-wave process of mass transport through the porous capillary wall." *Journal of Kaledney* 55 (1993): 109-113.
[22] El Shehawey, E. F., and S. Z. A. Husseny. "Effects of porous boundaries on peristaltic transport through a porous medium." *Acta Mechanica* 143, no. 3-4 (2000): 165-177.
[23] Rao, A. Ramachandra, and Manoranjan Mishra. "Peristaltic transport of a power-law fluid in a porous tube." *Journal of Non-Newtonian Fluid Mechanics* 121, no. 2-3 (2004): 163-174.
[24] Vajravelu, Kuppalapalle, S. Sreenadh, R. Hemadri Reddy, and K. Murugesan. "Peristaltic Transport of a Casson fluid in contact with a Newtonian Fluid in a Circular Tube with permeable wall." *International Journal of Fluid Mechanics Research* 36, no. 3 (2009): 244-254.
[25] Kothandapani, M., and S. Srinivas. "On the influence of wall properties in the MHD peristaltic transport with heat transfer and porous medium." *Physics Letters A* 372, no. 25 (2008): 4586-4591.
[26] Ellahi, Rahmat, M. Mubashir Bhatti, Arshad Riaz, and Mohsen Sheikholeslami. "Effects of magnetohydrodynamics on peristaltic flow of Jeffrey fluid in a rectangular duct through a porous medium." *Journal of Porous Media* 17, no. 2 (2014).
[27] Raza, Jawad, Fateh Mebarek-Oudina, and A. J. Chamkha. "Magnetohydrodynamic flow of molybdenum disulfide nanofluid in a channel with shape effects." *Multidiscipline Modeling in Materials and Structures* 15, no. 4 (2019): 737-757.
[28] Raza, Jawad, Fateh Mebarek-Oudina, and B. Mahanthesh. "Magnetohydrodynamic flow of nano Williamson fluid generated by stretching plate with multiple slips." *Multidiscipline Modeling in Materials and Structures* 15, no. 5 (2019): 871-894.
[29] Raza, Jawad, Mushayydha Farooq, Fateh Mebarek-Oudina, and B. Mahanthesh. "Multiple slip effects on MHD non-Newtonian nanofluid flow over a nonlinear permeable elongated sheet." *Multidiscipline Modeling in Materials and Structures* 15, no. 5 (2019): 913-931.
[30] Srivastava, L. M., V. P. Srivastava, and S. N. Sinha. "Peristaltic transport of a physiological fluid." *Biorheology* 20, no. 2 (1983): 153-166.
[31] Afsar Khan, A., R. Ellahi, and K. Vafai. "Peristaltic transport of a Jeffrey fluid with variable viscosity through a porous medium in an asymmetric channel." *Advances in Mathematical Physics* 2012, (2012): 1-15.
[32] Gudekote, Manjunatha, and Rajashekhar Choudhari. "Slip effects on peristaltic transport of Casson fluid in an inclined elastic tube with porous walls." *Journal of Advanced Research in Fluid Mechanics and Thermal Sciences* 43, no. 1 (2018): 67-80.
[33] Manjunatha, Gudekote, C. Rajashekhar, Hanumesh Vaidya, and K. V. Prasad. "Peristaltic mechanism of Bingham liquid in a convectively heated porous tube in the presence of variable liquid properties." *Special Topics & Reviews in Porous Media: An International Journal* 10, no. 2 (2019).
[34] Vaidya, Hanumesh, Rajashekhar Choudhari, Manjunatha Gudekote, and Kerehalli Vinayaka Prasad. "Effect of variable liquid properties on peristaltic transport of Rabinowitsch liquid in convectively heated complaint porous channel." *Journal of Central South University* 26, no. 5 (2019): 1116-1132.
[35] Vaidya, Hanumesh, C. Rajashekhar, G. Manjunatha, and K. V. Prasad. "Effect of variable liquid properties on peristaltic flow of a Rabinowitsch fluid in an inclined convective porous channel." *The European Physical Journal Plus* 134, no. 5 (2019): 231.
[36] Vaidya, Hanumesh, C. Rajashekhar, G. Manjunatha, and K. V. Prasad. "Peristaltic mechanism of a Rabinowitsch fluid in an inclined channel with complaint wall and variable liquid properties." *Journal of the Brazilian Society of Mechanical Sciences and Engineering* 41, no. 1 (2019): 52.